Biophysical Chemistry 253 (2019) 106214

Contents lists available at ScienceDirect

Biophysical Chemistry

journal homepage: www.elsevier.com/locate/biophyschem

Molecular dynamics simulations of membrane properties affected by plasma ROS based on the GROMOS force field

Yujia Hu, Tong Zhao*, Liang Zou, Xiaolong Wang, Yuantao Zhang

School of Electrical Engineering, Shandong University, Ji'nan, Shandong 250061, People's Republic of China

HIGHLIGHTS

- Concentration affects the distribution of ROS at the membrane-water interface.
- Under plasma treatment, the energy barrier of HO_2 translocation across the membrane decreases significantly.
- The unsaturated regions of the phospholipid and cholesterol are susceptible to oxidation by O_2 and HO_2, respectively.
- The distribution of plasma ROS will cause the change of membrane morphology.
- The MD results give insight into the plasma sterilization process.

GRAPHICAL ABSTRACT

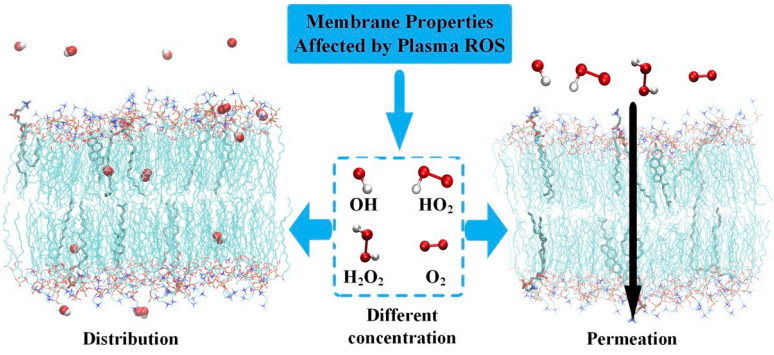

ARTICLE INFO

Keywords:
Cold atmospheric plasma
Sterilization
Reactive oxygen species
Cell membrane
Molecular dynamics

ABSTRACT

Cold atmospheric plasma (CAP) has attracted substantial attention in the field of medical disinfection because its main components, reactive oxygen species (ROS), have a strong destructive effect on various cell components. The cell membrane plays an important role in maintaining proper cellular function by blocking harmful substances such as ROS. In this paper, we used molecular dynamics simulations to study the behaviour of different ROS at the membrane-water interface. The results showed that the cell membrane presented a weak barrier to hydrophobic ROS (O_2) but effectively prevented hydrophilic ROS (OH, HO_2, H_2O_2) from entering the cell. The plasma treatment significantly enhanced the permeability of the cell membrane to HO_2, while the energetic barrier to other types of ROS changed only slightly. O_2 very likely stopped in the centre of the lipid bilayer when crossing the membrane and there attacked the unsaturated region of the phospholipid. Cholesterol was most likely oxidized by HO_2, causing a condensing effect that destroyed the integrity and fluidity of the cell membrane. The study also found that large amounts of ROS decreased the thickness of the cell membrane, and the phospholipid arrangement became disordered.

1. Introduction

In recent years, cold atmospheric plasma (CAP) has become an important topic in the fields of chemistry and biology, with potential applications such as pollution degradation, cancer treatment, and sterilization [1–3]. In particular, with improving medical standards, the drawbacks of traditional disinfection methods have attracted increasing attention [4], and the new CAP sterilization method has many advantages over traditional sterilization methods [5–7]. CAP is a mixture of electrons, ions, atoms and free radicals, and the whole is electrically

* Corresponding author.
E-mail address: zhaotong@sdu.edu.cn (T. Zhao).

https://doi.org/10.1016/j.bpc.2019.106214
Received 7 March 2019; Received in revised form 25 June 2019; Accepted 25 June 2019
Available online 26 June 2019

neutral. Studies have shown that the main types of free radicals are hydroxyl radicals (OH) [8], hydroperoxide radicals (HO_2) [9], singlet oxygen ($^1O_2$) [10], etc. These substances exhibit strong nanotoxicity and have a strong destructive effect on the structure of bacterial substances [11].

The bactericidal process of plasma sterilization is very complex and involves affecting gene expression, blocking signalling pathways, reducing metabolic levels, causing oxidative stress and exerting other effects [12]. To date, a large body of literature has attempted to explain the mechanism of plasma sterilization. Cell membranes, a barrier protecting proteins and nucleic acids, can block reactive oxygen species (ROS) from entering the interior of cells. However, due to the strong fluidity of the cell membrane, high-permeability ROS can enter the cell interior with relative ease [13,14]. Plasma treatment can result in intracellular ROS concentrations that exceed the capacity of the cell defence systems, causing the cells to suffer oxidative stress. The antioxidant system in the cells might become unable to cope with the damage sustained by the cells, resulting in damaged DNA going unrepaired, eventually leading to cell death [15]. Therefore, the key factor in bacterial inactivation is the permeability of free radicals into the bacterial membrane [16]. Experiments have shown that in an acidic environment, the combination of O_2^- and H ions causes an increase in the concentration of HO_2, which, due to its high permeability into the cell membrane, significantly enhances the killing effect of plasma on bacteria [16]. H Zhang found that long-lived H_2O_2 molecules cause a modification of the secondary structure and polymerization of the peptide chains, and increasing concentration of H_2O_2 leads to a reduced alpha-helix content, thereby inactivating the bacteria [17]. JG Birmingham identified small acid-soluble proteins (SASPs) in bacterial spores by mass spectrometry and found that plasma acts rapidly and causes spore inactivation [18]. Furthermore, due to the special structure of the individual phospholipid molecules (head hydrophilicity and tail hydrophobicity), some of the ROS accumulate at a certain position in the lipid bilayer during translocation across the membrane, resulting in a 'membrane lens effect' [19]. At the same time, phospholipids and cholesterol, the main components of the cell membrane, are also attacked by ROS, which affects the fluidity and integrity of the membrane [20]. In addition, the distribution of ROS is closely related to the working efficiency of natural antioxidants such as β-carotene and α-tocopherol contained in cell membranes [21].

To date, there has been a preliminary study on the distribution and permeability of ROS at the membrane-water interface [22]. The depth of entry of different ROS into the cell membrane can be detected using fluorescent probes [23]. However, due to the fluidity of the cell membrane itself, the experimental results have high uncertainty [21]. With the development of computational chemistry, molecular dynamics simulations provide a method to analyse the interaction between the cell membrane and ROS at the atomic level. RM Cordeiro calculated the various ROS parameters for the first time to accurately analyse the behaviours of the ROS at the membrane-water interface [21]. Recently, more complex models have been constructed to study the distribution of cholesterol, ceramides and other substances in the cell membrane, as well as the permeability of ROS in natural membranes [24,25]. In addition, the effects of cholesterol and lipid oxidation on cell membrane morphology and changes in permeability were also demonstrated by molecular dynamics simulations [26–29]. The article explains the selective treatment of cancer cells by plasma because the increase in the proportion of cholesterol increases the difficulty of ROS translocation across the membrane [29]. Although many previous studies have comprehensively analysed the behaviour of ROS, the system is often the natural environment, and the amount of ROS in cells is very small [21]. Plasma treatment, as a new type of bactericidal method, can produce high concentrations of ROS near the cell membrane in a short period of time, which inevitably affects the distribution of ROS and its oxidation of cholesterol and phospholipids. Although there have been many studies on the effects of oxidation on cell membranes, little is known about the effect of concentration on the ROS distribution and permeability.

Based on the above considerations, this paper focuses on changes in the permeability of cell membranes to different ROS (O_2, HO_2, OH, H_2O_2) under natural conditions and under plasma treatment. These conclusions can guide us to change the concentration and proportion of various ROS in the plasma to improve its permeability. At the same time, the distribution of the main components (cholesterol, phospholipid) in the cell membrane was studied, and the probability of their oxidation can be calculated by integrating the result with the distribution of ROS. The conclusions provided in this study can guide future improvements in the sterilization efficiency by changing the concentration of key ROS in the plasma. In addition to sterilization, plasma with higher permeability provides important information for cancer treatment, wound healing, etc.

2. Computational methods and simulation details

2.1. Cell membrane structure

Phospholipdds are the main constituent of the cell membrane, and a cholesterol inlay maintains both rigidity and fluidity. In bacterial cell membranes, the most common phospholipid molecule is 2-oleoyl-1-palmitoyl-sn-glycero-3-phosphocholine (POPC). Fig. 1 shows the chemical structure of POPC using the parameters of Poger and Mark [24] (Fig. 1B) and the chemical structure of cholesterol (CHO) using the parameters of Antenor (Fig. 1C) [27].

Fig. 1A shows a cell membrane model with a cholesterol/phospholipid molar ratio of 50%, generated using PACKMOL [31]. The model is composed of 128 phospholipid molecules and 64 cholesterol molecules surrounded by 5000 water molecules. Due to the special structure of POPC (hydrophilic head, hydrophobic tail), the molecule forms a two-layer structure in water, and cholesterol is vertically arranged between the phospholipid molecules [27].

2.2. Derivation of interaction parameters

The simulation was based on the GROMOS 53A6 force field in GROMACS, which is suitable for describing the distribution of molecules within a large system [21,30]. The parameters of this simplified lipid structure were developed by Poger and Mark [24]. The properties of the cell membrane constructed with this simplified model are in very good agreement with the experimental results, including area per lipid, volume per lipid and the deuterium order parameters. On the other hand, the hydration of the headgroups and tailgroups was consistent with the experimental results, and these values are very important for the distribution of ROS analogues at the membrane-water interface.

The parameters for O_2, HO_2, OH, and H_2O_2 were adapted from the literature, and the parameters for bonds, angles and torsions were modified for use in gromos53A6 force field [32,33]. As the distribution of these ROS analogues at the membrane-water interface is the focus of research, their van der Waals interactions and partial charges are adjusted to match their hydration free energies to the experimental data [21]. Furthermore, experiments prove that the radical anionic form of O_2 and ground-state O_2 have similar partition coefficients between water and hydrophobic media, indicating that omitting the unpaired electrons from consideration does not affect the distribution of O_2 at the membrane-water interface [34,35]. However, if the system solvent is changed, the parameters of these ROS analogues will no longer be applicable to the new system.

2.3. Simulation details

2.3.1. Simulation of the ROS distribution

We studied the ROS distributions between an aqueous phase and a POPC bilayer by increasing the density and obtaining different partial densities to elucidate the relationship between the ROS density and its

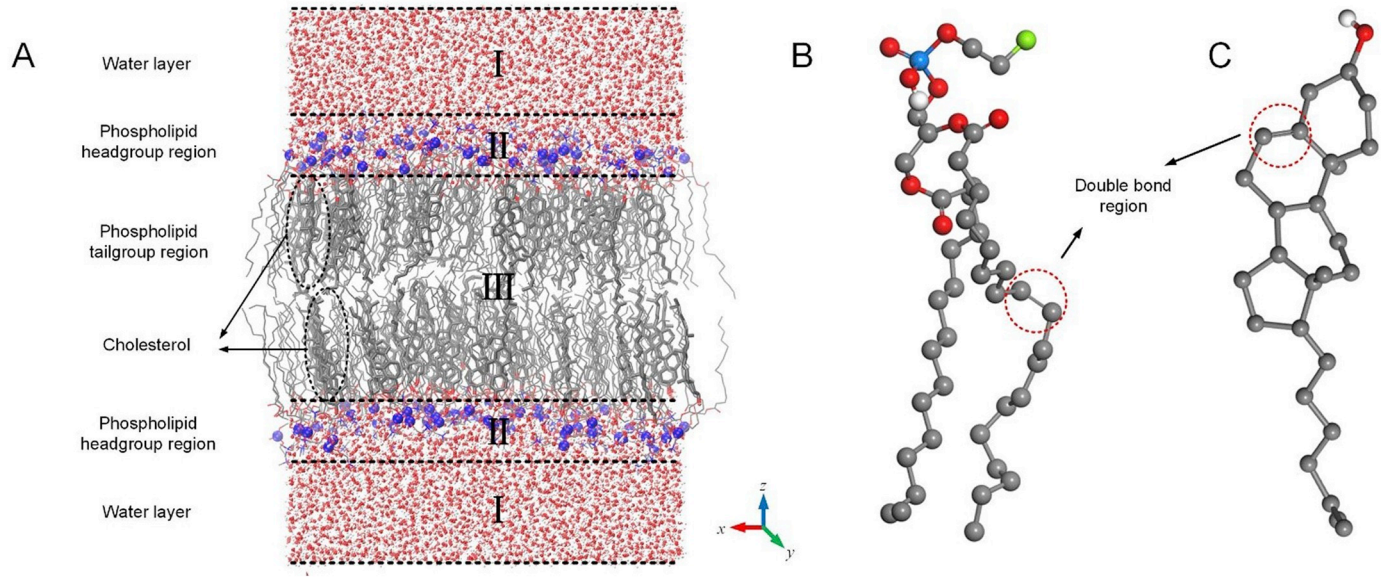

Fig. 1. (A) A lipid bilayer model after 100 ns of equilibration, including 128 POPC molecules, 54 cholesterol molecules and 5000 water molecules. The model is divided into three main regions: the water layer (I), phospholipid headgroup region (II), and phospholipid tailgroup region (III). The oxygen atoms and lipid tails are shown in red and grey. To make the interface between the membrane and water clearer, the phosphorus (blue) atoms are depicted by larger beads. Cholesterol molecules are indicated by black circles. (B) Schematic illustration of POPC. The hydrogen and nitrogen atoms are shown in white and green, respectively. The same colour code is used in other figures in this paper. (C) Schematic illustration of cholesterol. The double bond regions of cholesterol and POPC are indicated by red circles. (For interpretation of the references to colour in this figure legend, the reader is referred to the web version of this article.)

distribution. An initial model of various ROS analogues was established to study the distribution at the membrane-water interface. Referring to previous research on the behaviour of ROS at the membrane-water interface [21], to improve the calculation accuracy and the credibility [36], the model addressed a higher ROS concentration than can be generated in general plasma. This setting can improve the accuracy and efficiency of the calculation with minimal impact on the correctness of the results [36]. To create multiple models at 1%, 2% and 3% molar concentrations, 50, 100 and 150 various ROS analogues, respectively, were placed together with a pre-equilibrated phospholipid bilayer. After the initial configuration was generated using PACKMOL [31], system energy minimization was performed using the steepest descent method, and a 30 ns simulation with constant number, pressure, and temperature (NPT) was performed. The temperature was controlled to 310 K by applying a Nose-Hoover thermostat, and the pressure was controlled to 1 bar by using the Parrinello-Rahman method [37,38]. A 100 ns molecular dynamics simulation was performed to ensure that the system reached a good equilibrium state, and then the density distribution of the ROS analogues in the z-axis direction was counted. To improve the accuracy of the simulation, a separate coupling group was used for the ROS analogues, lipids, cholesterol and water. The time step was 2 fs, and a spanning Verlet scheme was used [39,40]. To maintain the cell membrane integrity, periodic boundary conditions were used. The partial densities of various ROS analogues were averaged after four repetitions of the simulation.

2.3.2. Analysis of cell membrane properties

Due to the strong fluidity of the cell membrane, the external environment can easily change in thickness and area, affecting the permeability to ROS. Studies have shown that the distribution of some ROS in the lipid bilayer affects the distribution of phospholipids and cholesterol [27]. The effect of ROS on the cell membrane thickness and area was analysed using the last 10 ns simulated by the distribution of the ROS analogues. The bilayer thickness was obtained by calculating the average position of the upper and lower phosphorus atoms on the z-axis.

2.3.3. Calculation of the free energy profile

We calculated the free energy profiles for the translocation of ROS analogues across the membrane at different ROS densities to study how concentration changes affect the permeability of various ROS. The free energy change during the whole process of ROS passing through the cell membrane can be calculated by the umbrella sampling method [41]. The initial structures were picked randomly from the last 10 ns of the ROS analogue distribution simulation. Then, suitable ROS were selected to move from the bulk water to the centre of the lipid bilayer through a 3 Å distance, a process divided into 60 umbrella windows. A force of 1000 kJ/mol was used to move the ROS along the z-axis while allowing them to move freely in the xy plane. After a 500 ps equilibration using the steepest descent method, a 3 ns NPT ensemble and a 2 ns molecular dynamics simulation were performed. The free energy profiles of various ROS analogues were obtained by weighted histogram analysis using the gmx wham tool [42]. Each ROS was simulated using ten different initial configurations, and the final free energy profile was obtained after averaging. The total computing time was more than 20,000 ns, consuming a large amount of computing resources.

3. Results and discussion

3.1. Distribution of ROS and cholesterol

During the sterilization process, the plasma first contacts the cell membrane and destroys its main components. Fig. 2 illustrates the changes in various ROS analogue distributions at the membrane-water interface caused by an increase in the concentration. When calculating the equilibrium distribution, the rate of ROS flowing into the bilayer is the same as the rate flowing out of the bilayer, which indicates that the systems are close to 'steady state'. In the aqueous phase and lipid bilayers, the behaviour of various ROS analogues is mainly affected by hydrogen bonding, van der Waals interaction and other intermolecular interactions [44]. Because hydrogen bonding is stronger than van der Waals interaction, it plays a major role in the distribution of ROS. Because O_2 is hydrophobic and is not bound by hydrogen bonding in water, it easily diffuses from a high-density region to a low-density

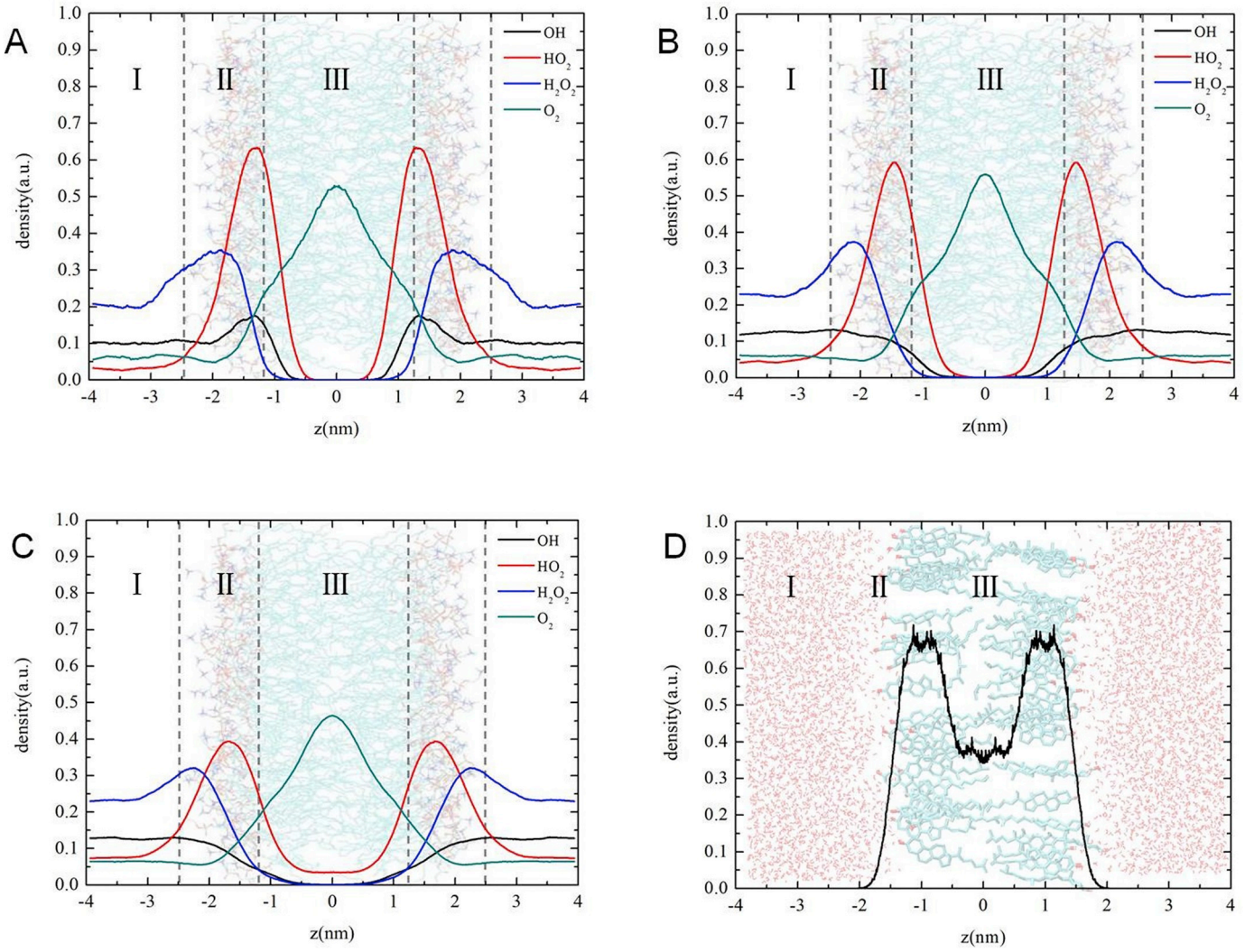

Fig. 2. Distributions of various ROS analogues at 1% (A), 2% (B), and 3% (C) molar concentrations. The water layer and cholesterol molecules are omitted in the background. Distribution of cholesterol molecules (D). Phospholipid molecules are omitted in the background.

region. Because the interior of the lipid bilayer is low in atomic density due to the inaccessibility of water molecules, most O_2 will penetrate into it and remain stable at the centre. Integration shows that the internal concentration of O_2 is approximately 3.5 times that of water on average, which is the same as that measured using the spin-label method [45].

Hydrogen bonds formed with the water layer play a decisive role in their distribution of all hydrophilic ROS analogues, including OH, HO_2 and H_2O_2. As shown in Table 1, due to the similar number of hydrogen bonds formed, the maximum values of the OH and HO_2 partial densities occur at the same x-coordinate, which means they tend to stay in the same position in the cell membrane. However, the excess oxygen atoms of HO_2 form stronger van der Waals interactions with lipids, as shown in Table 2, making the density of HO_2 in the phospholipid headgroup region one order of magnitude higher than that of OH. Compared to OH and HO_2, H_2O_2 forms more than twice the number of hydrogen bonds [46], which positions it farther from the centre of the lipid bilayer.

Table 1
H-bonds between ROS analogues and water.

Species	Number of H-bonds
OH	0.961
HO_2	1.241
H_2O_2	3.763
O_2	0

Table 2
The van der Waals interactions between ROS analogues and bilayer.

Species	van der Waals interactions
OH	−0.7 kJ/mol
HO_2	−4.9 kJ/mol
H_2O_2	−1.4 kJ/mol
O_2	−6.7 kJ/mol

The distribution of ROS affects the oxidation efficiency of cholesterol. To demonstrate this point, we simulated the distribution of cholesterol in the lipid bilayer, as shown in Fig. 2D. Compared to O_2, cholesterol is mainly distributed in the tailgroup region due to its long chain length. Moreover, because the hydroxyl group (-OH) of cholesterol forms a hydrogen bond with the phospholipid group, the cholesterol and the phospholipid tail lie essentially parallel. Although O_2 has the most overlap with cholesterol in terms of distribution, it mainly contacts a relatively stable carbon chain, which does not readily initiate an oxidation reaction. From the perspective of cholesterol peroxide formation, although HO_2 is hydrophilic, its oxidation efficiency is closer to that of O_2.

3.2. Effect of ROS concentration on its distribution

The ROS concentration generated by plasma is affected by many factors, such as gas type, voltage, and frequency [47]. Fig. 2 shows the distribution of ROS analogues at different concentrations. The distribution of O_2 did not change significantly when the molar concentration of ROS analogues increased from 1% to 2%. Because the atomic concentration inside the lipid bilayer is still much lower than that in the aqueous phase, a large amount of O_2 is still distributed in the membrane interior. As the concentration increases further, and the amount of O_2 in the centre of the lipid bilayer becomes saturated. At this time, the atomic density inside the lipid bilayer and the atomic density in the aqueous phase gradually become similar, and the permeability of O_2 is weakened.

In hydrophilic ROS analogues, the distribution of HO_2 did not change notably when the molar concentration increased from 1% to 2%. However, the density of OH at the headgroup region decreased significantly, resulting in a downward trend in the entire profile from the aqueous phase to the centre of the lipid bilayer. This trend occurs because the space in the phospholipid headgroup region is limited, HO_2 is more easily distributed than OH in this region due to the stronger van der Waals interaction, resulting in a large amount of OH being extruded into the aqueous phase. As the concentration increased further, the peak of the HO_2 distribution curve began to decrease, while the profile in the aqueous phase increased significantly. Because the space in the headgroup region already contains more HO_2, the van der Waals interaction between the other HO_2 molecules was weakened. Most of these unbound HO_2 remained randomly distributed in the aqueous phase, while a small amount entered the lipid bilayer.

The accumulation of large amounts of ROS leads to changes in the cell membrane structure, as described in previous studies [25]. As shown in Fig. 3, a large amount of OH and HO_2 increased the distance between adjacent phospholipid molecules in the horizontal plane. Compared with normal cell membranes, the bilayer area (per lipid) increased slightly under plasma treatment [24]. When the molar concentration of ROS analogues was increased from 1% to 3%, the bilayer area (per lipid) increased from $0.652 \pm 0.1\ nm^2$ to $0.683 \pm 0.08\ nm^2$, which indicates that the presence of ROS increases the bilayer area. At the same time, OH and HO_2 began to appear inside the lipid bilayer, which can also be explained by the increase in lipid area. As the distance between adjacent phospholipid molecules increases, more voids appear in the cell membrane to accommodate the ROS.

In addition, an increase in the ROS analogue concentration results in a decrease in the thickness of the lipid bilayers from 3.65 ± 0.07 nm to 3.57 ± 0.03 nm, which is associated with an increase in the concentration of ROS in the headgroup region. Recent studies have shown that if the cell membrane structure changes, resulting in an increase in water density at the headgroup region, the lipid atoms will be squeezed towards the centre, thereby reducing the thickness of the lipid bilayer [48]. The simulations show that the increase in ROS concentration has a similar effect to the increase in water density. Because H_2O_2 can double the number of hydrogen bonds in OH and HO_2 in water, the distribution in the aqueous phase is the most stable, and the partial densities of H_2O_2 change very little with concentration [46]. Even if the lipid area is increased to increase the internal voids, H_2O_2 cannot translocate into the lipid bilayer due to strong hydrogen bonding interactions with water.

3.3. Effect of ROS concentration on cholesterol and phospholipid oxidation

To analyse the role of various ROS in the oxidation of phospholipids and cholesterol, it is important to calculate their probability of contact with the double bond region. Due to the fluidity and disorder of the membrane, there is a significant overlap between the distribution of various ROS and the double bond regions. Therefore, by calculating the integral of the overlap of the ROS and double bond region distribution, the oxidation probability of various ROS can be calculated. This probability is given by [21]:

$$T = \frac{1}{\rho^{\infty}_{ROS}} \int \rho(z) \cdot \rho_{ROS}(z) dz \tag{1}$$

where ρ^{∞}_{ROS} is the concentration of various ROS in a large volume of water, and $\rho_{ROS}(z)$ and $\rho(z)$ represent the distribution of specific ROS and double bond regions, respectively. The probabilities of various ROS analogues in contact with unsaturated regions of phospholipid molecules are shown in Table 3 and Fig. 4. Because the probabilities of various ROS differ by several orders of magnitude, the results are represented by logarithmic coordinate axes. The simulation results are

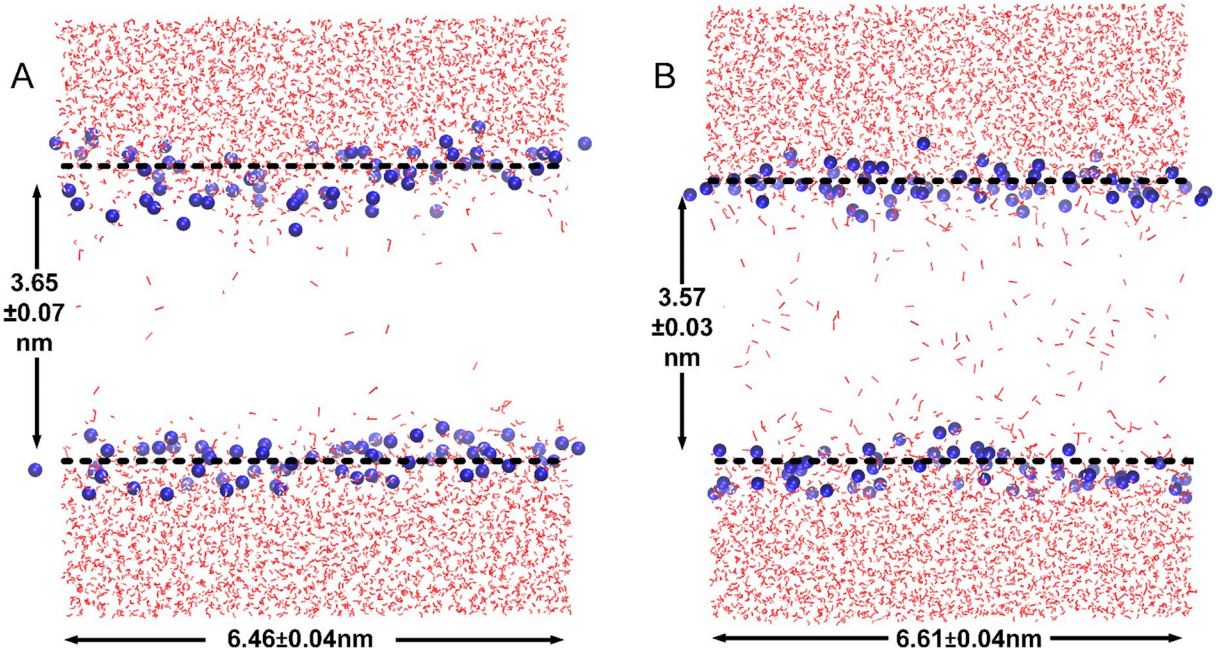

Fig. 3. Effect of ROS on the cell membrane area and thickness at molar concentrations of 1% (A) and 3% (B). Note that the lipid tails and cholesterol molecules in the figure are not shown.

Table 3
Oxidation probability of various ROS analogues in unsaturated regions of phospholipid molecules.

Molar concentrations	Unsaturated regions of phospholipid molecules				Unsaturated regions of cholesterol molecules			
	OH	HO_2	H_2O_2	O_2	OH	HO_2	H_2O_2	O_2
0.5%	0.15 ± 0.09	5.68 ± 0.34	0.008 ± 0.006	5.29 ± 0.32	1.74 ± 0.29	21.14 ± 1.45	0.71 ± 0.11	2.9 ± 0.31
1%	0.51 ± 0.18	4.99 ± 0.51	0.426 ± 0.213	9.74 ± 0.56	2.05 ± 0.39	36.69 ± 2.09	0.99 ± 0.09	5.72 ± 0.61
1.5%	0.31 ± 0.11	8.87 ± 0.67	0.016 ± 0.014	15.08 ± 0.43	2.53 ± 0.12	56.17 ± 1.87	1.06 ± 0.13	8.13 ± 0.41
2%	0.75 ± 0.13	12.98 ± 0.89	0.164 ± 0.121	18.36 ± 0.72	2.73 ± 0.15	56.01 ± 3.59	1.58 ± 0.31	11.41 ± 0.86
2.5%	0.53 ± 0.23	14.78 ± 0.79	0.027 ± 0.021	25.13 ± 0.81	4.22 ± 0.21	93.62 ± 5.42	1.76 ± 0.19	13.55 ± 0.72
3%	1.63 ± 0.21	15.51 ± 0.56	0.618 ± 0.278	28.09 ± 0.65	3.49 ± 0.44	75.99 ± 7.33	1.55 ± 0.15	17.92 ± 1.12

consistent with the results of using molecular probes to detect the depth of various ROS entering the phospholipid bilayer [23,49]. In the case of phospholipids, the unsaturated region is located in the middle of the tail chain and has the highest probability of contact with O_2 distributed in the centre of the lipid bilayer. A small amount of HO_2 molecules entering the phospholipid tailgroup region are derived from radicals by extracting hydrogen atoms, thereby destroying the double bond region [50]. OH and H_2O_2 are basically negligible for the oxidation of phospholipids due to the barrier function of the cell membrane. As the concentration increases, the oxidization probability of all ROS is improved. However, it is worth noting that the The increase in O_2 is more obvious, indicating that it plays a more important role in the oxidation of phospholipids.

The double bond regions of cholesterol lie close to the water layer and parallel to the phospholipid. Fig. 4(B) shows that HO_2 has the highest probability of contact with the unsaturated positions, one order of magnitude higher than OH and H_2O_2, which can be explained by the distribution of ROS analogues and cholesterol. Due to the strong van der Waals interactions of the phospholipid headgroups, the distributions of HO_2 and the cholesterol head exhibit greater overlap. Notably, increasing the concentration, the oxidation probability of hydrophobic ROS (O_2) increases, while the growth rates of hydrophilic ROS (H_2O_2, HO, HO_2) gradually slow down.

The relative reactivity of ROS analogues is also an important factor affecting membrane oxidation. HO_2 and the radical anionic form of O_2 can initiate lipid peroxidation [51]. Although H_2O_2 is a two-electron oxidant, it reacts poorly or not at all with most biological molecules [52]. Therefore, the role of H_2O_2 in the oxidation of lipids and cholesterol can be ignored because of its low contact probability and low reactivity. The amount of OH in the lipid bilayer is two orders of magnitude lower than that of the other ROS and has greater randomness, but the reaction rate constants of OH for biological components are extremely high (10^7–$10^9\ m^{-1}\ s^{-1}$) [53]. Therefore, the role of OH in interactions between lipids and cholesterol cannot be fully assessed.

3.4. Effect of ROS on lipid bilayer permeability

Short-term plasma treatment does not break the cell membrane, and a large amount of ROS remains stable at the membrane-water interface, which in turn affects the cell membrane permeability. Fig. 5 shows the translocation of ROS analogues across the membrane under natural conditions (A) and plasma treatment conditions (B). The higher the free energy is, the more difficult it is for ROS analogues to translocate across the membrane and react with proteins, nucleic acids and other substances. The free energy values of all ROS analogues are given in Table 4.

Under natural conditions, the bacterial cells exist in the natural environment without plasma treatment, and intracellular ROS are produced by cells for redox reactions to ensure normal functioning. In this case, the concentration of ROS in the cells is extremely low, so only one ROS analogue was placed in the model of natural conditions for translocation across the membrane. For hydrophobic O_2, the free energy profile tended to decrease from the water layer to the centre of the lipid bilayer, which indicates that O_2 can easily translocate across a phospholipid monolayer. The membrane acts as an effective barrier to protect internal substances from all hydrophilic ROS. For H_2O_2, the transfer free energy is approximately 35.1 ± 3.3 kJ/mol, which is essentially the same as the 36.8 kJ/mol measured in a previous study [54]. As shown in Table 4, the transfer free energy of HO_2 and OH is approximately half that of H_2O_2. Combining this information with analysis of the distribution of these ROS in the cell membrane, it can be concluded that hydrogen bonding is the main mechanism of preventing translocation across the membrane. Notably, as shown in Table 5, hydrogen bonds can also form between the hydrophilic ROS and phosphate groups, and OH and HO_2 have a free energy minimum at the headgroup region. However, due to the stronger van der Waals

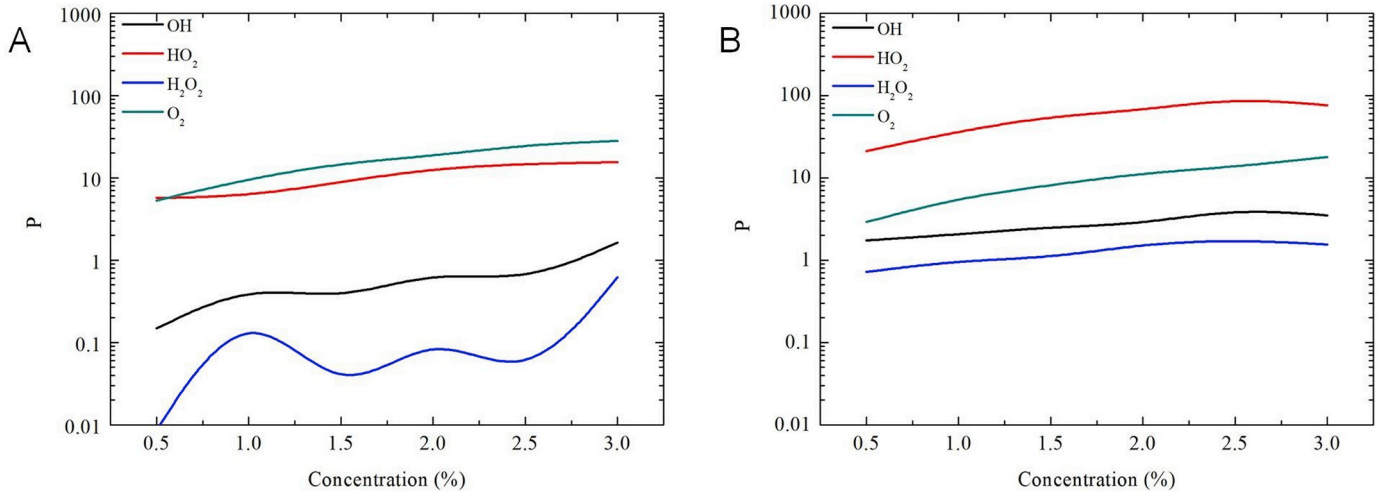

Fig. 4. Oxidation probability of various ROS analogues in unsaturated regions of phospholipid molecules (A) and cholesterol molecules (B).

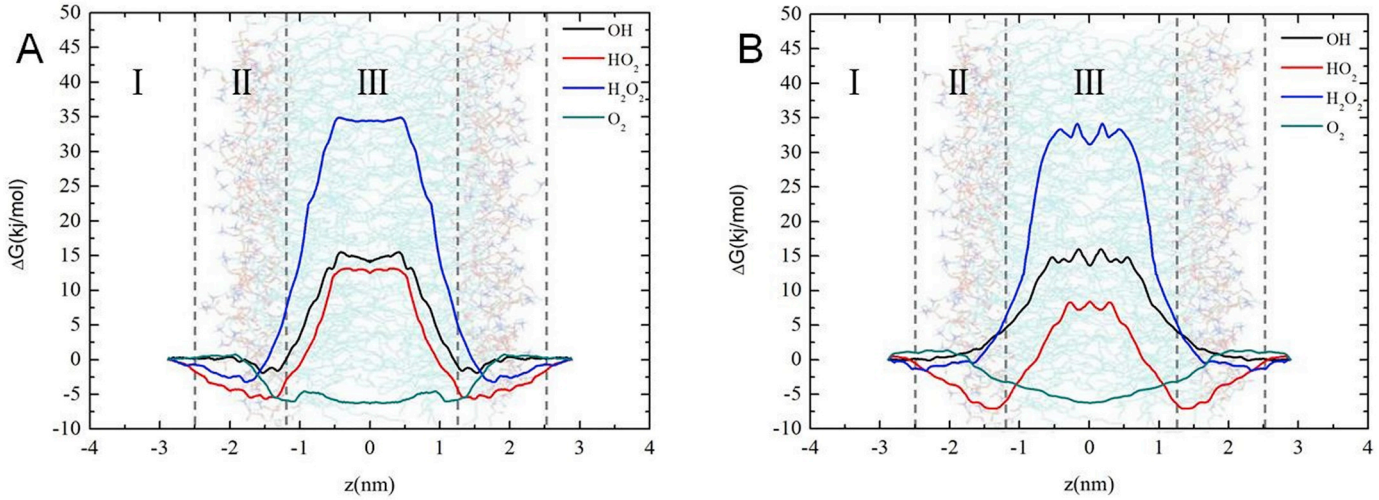

Fig. 5. Free energy profiles of various ROS analogues passing through the cell membrane under natural conditions (A) and plasma treatment conditions (B).

Table 4
The free energy values for the translocation of all ROS analogues across the membrane under natural conditions and plasma treatment conditions.

ROS	Under natural conditions	Under plasma treatment conditions
OH	15.6 ± 1.6 kJ/mol	15.3 ± 1.3 kJ/mol
HO_2	13.5 ± 1.7 kJ/mol	10.2 ± 1.9 kJ/mol
H_2O_2	35.1 ± 3.3 kJ/mol	34.2 ± 2.1 kJ/mol
O_2	−5.1 ± 0.7 kJ/mol	−5.2 ± 0.8 kJ/mol

Table 5
H-bonds between ROS analogues and phosphate groups.

Species	Number of H-bonds
OH	0.165
HO_2	0.264
H_2O_2	0.588
O_2	0

interaction with the phosphate groups, HO_2 can maintain a deeper position in the lipid bilayer than OH.

In contrast to the natural environment, the bacterial cell membrane after plasma treatment is filled with a large amount of ROS analogues. These ROS affect hydrophobic and van der Waals interactions, in turn affecting the permeability of the cell membrane. To illustrate this effect, we calculated the free energy profiles of various ROS analogues at 3% molar concentration, as shown in Fig. 5(B). Combining the distribution of various ROS analogues, we expect similar but less obvious results at low concentrations. Because O_2 cannot form hydrogen bonds, the ROS at the membrane-water interface have little effect on the membrane permeation process. However, the rate of decline in free energy during membrane permeation is closer, which is attributed to more uniform atomic density in the lipid bilayer. The free energy for H_2O_2 permeation is estimated to be 34.2 ± 2.1 kJ/mol, which is essentially the same as the value of 35.1 ± 3.3 kJ/mol obtained under natural conditions. Notably, the increase in the free energy of H_2O_2 at the position of the phospholipid head is slowed down, indicating that it can penetrate more deeply into the lipid bilayer, as shown in Fig. 2C. An increase in the concentration of HO_2 promotes an overall decrease in its free energy and facilitates translocation from the phospholipid headgroup region to the tailgroup region, which explains the conclusions drawn from previous experiments. In contrast to that of HO_2, the free energy profile of OH shows an upward trend, reaching the maximum free energy at the centre of the lipid bilayer. Plasma treatment does not impair the barrier effect of the cell membrane against OH but facilitates a more even distribution in the aqueous phase.

4. Conclusion

In this paper, we used united-atom force fields to simulate the behaviour of various ROS at the membrane-water interface and to study membrane morphology and permeability changes at the microscopic level. The results showed that for different types of ROS and phospholipids, the oxidation probability of cholesterol is very different. The arrangement of phospholipids in the cell membrane is also affected by the ROS generated by the plasma.

(1) Concentration affects the distribution of ROS at the membrane-water interface, thereby affecting the probability of contact with phospholipids and cholesterol, and the efficiency of plasma destruction of the cell membranes.
(2) Hydrophobic O_2 can easily penetrate into and remain within the lipid bilayer, resulting in the highest probability of contact with the unsaturated region of the phospholipid and thus playing the most important role in oxidation. The double bond region of cholesterol is the most susceptible to oxidation by HO_2.
(3) The ROS at the headgroup region of the phospholipid decrease the thickness of the cell membrane, and the ROS inside the lipid bilayer cause an alignment between the phospholipids, thereby increasing the membrane area.
(4) Under natural conditions, hydrophobic O_2 is most likely to enter the interior of the cell, while the lipid bilayer forms a strong barrier to hydrophilic ROS (OH, HO_2, H_2O_2). Among them, H_2O_2 has the highest barrier energy due to hydrogen bonding, while OH and HO_2 are basically similar. Under plasma treatment, the energy barrier of HO_2 decreases significantly, while the other types of ROS do not change greatly.

This paper describes the permeation and distribution of various ROS in the cell membrane at the microscopic level and calculates the oxidation probability of phospholipids and cholesterol. These results are jointly proven and complement existing experiments. Our simulations improve the understanding of plasma destruction of the cell membrane and the accumulation of intracellular ROS, which can guide the variation in ROS concentration in experiments to increase the degree of oxidative stress and the rate of cell membrane destruction, thereby improving the efficiency of plasma sterilization. Finally, we can also report that united-atom force fields are an effective means of understanding the interaction between plasma and cells.

Acknowledgements

This work was supported by the National Natural Science Foundation of China (Project No. 11675095) and the Fundamental Research Funds of Shandong University (Project No. 2017JC017).

References

[1] M. Keidar, E. Robert, Preface to special topic: plasmas for medical applications, Phys. Plasmas 22 (2015) 121901.
[2] D.B. Graves, Low temperature plasma biomedicine: a tutorial reviewa, Phys. Plasmas 21 (2014) 080901.
[3] A. Maciuca, C. Batiot-Dupeyrat, J.M. Tatibouët, Synergetic effect by coupling photocatalysis with plasma for low VOCs concentration removal from air, Appl. Catal. B 125 (2012) 432.
[4] M. Laroussi, Nonthermal decontamination of biological media by atmospheric-pressure plasmas: review, analysis, and prospects, IEEE T. Plasma Sci. 24 (2002) 1181–1191.
[5] S. Lerouge, M.R. Wertheimer, L. Yahia, Plasma sterilization: a review of parameters, mechanisms, and limitations, Plasmas Polym. 6 (2001) 175–188.
[6] H. Liu, J. Chen, L. Yang, Y. Zhou, Long-distance oxygen plasma sterilization: effects and mechanisms, Appl. Surf. Sci. 125 (2008) 432–438.
[7] S. Lerouge, M.R. Wertheimer, R. Marchand, M. Tabrizian, L. Yahia, Effect of gas composition on spore mortality and etching during low-pressure plasma sterilization, J. Biomed. Mater. Res. 51 (2000) 128.
[8] B.R. Locke, M. Sato, P. Sunka, M.R. Hoffmann, J.S. Chang, Electrohydraulic discharge and nonthermal plasma for water treatment, Ind. Eng. Chem. Res. 45 (2006) 882–905.
[9] S. Ikawa, K. Kitano, S. Hamaguchi, Effects of pH on bacterial inactivation in aqueous solutions due to low-temperature atmospheric pressure plasma application, Plasma Process. Polym. 7 (2010) 33–42.
[10] D.X. Liu, M.Z. Rong, X.H. Wang, F. Iza, M.G. Kong, Main species and physico-chemical processes in cold atmospheric-pressure He + O_2 plasmas, Plasma Process. Polym. 7 (2010) 846–865.
[11] M. Laroussi, D.A. Mendis, M. Rosenberg, Plasma interaction with microbes, New J. Phys. 5 (2003) 41.
[12] O. Lunov, V. Zablotskii, O. Churpita, A. Jäger, L. Polívka, E. Syková, A. Dejneka, S. Kubinová, The interplay between biological and physical scenarios of bacterial death induced by non-thermal plasma, Biomaterials 82 (2016) 71–83.
[13] M. Afri, H.E. Gottlieb, A.A. Frimer, Superoxide organic chemistry within the liposomal bilayer, part II: a correlation between location and chemistry, Free Radic. Biol. Med. 32 (2002) 605–618.
[14] A. Gamliel, M. Afri, A.A. Frimer, Free Radic. Biol. Med. 44 (2008) 1394–1405.
[15] R.N. Ma, H.Q. Feng, Y.D. Liang, Q. Zhang, Y. Tian, B. Su, An atmospheric-pressure cold plasma leads to apoptosis in Saccharomyces cerevisiae by accumulating intracellular reactive oxygen species and calcium, J. Phys. D. Appl. Phys. 46 (2013) 1.
[16] E. Takai, S. Ikawa, K. Kitano, J. Kuwabara, K. Shiraki, Molecular mechanism of plasma sterilization in solution with the reduced pH method: importance of permeation of HOO radicals into the cell membrane, J. Phys. D. Appl. Phys. 46 (2013) 295402.
[17] H. Zhang, Z. Xu, J. Shen, X. Li, L. Ding, J. Ma, Y. Lan, W. Xia, C. Cheng, Q. Sun, Z. Zhang, P.K. Chu, Effects and mechanism of atmospheric-pressure dielectric barrier discharge cold plasma on lactate dehydrogenase (LDH) enzyme, Sci. Rep. UK 5 (2015) 10031.
[18] J.G. Birmingham, Mechanisms of bacterial spore deactivation using ambient pressure nonthermal discharges, IEEE T. Plasma Sci. 32 (2004) 1526–1531.
[19] X. Liu, M.J. Miller, M.S. Joshi, D.D. Thomas, J.R. Lancaster, Accelerated reaction of nitric oxide with O2 within the hydrophobic interior of biological membranes, Proc. Natl. Acad. Sci. U. S. A. 95 (1998) 2175–2179.
[20] A. Reis, M.R. Domingues, F.M. Amado, A.J. Ferrer-Correia, P. Domingues, Radical peroxidation of palmitoyl-lineloyl-glycerophosphocholine liposomes: identification of long-chain oxidised products by liquid chromatography-tandem mass spectrometry, Biomed. Chromatogr. 19 (2010) 129–137.
[21] R.M. Cordeiro, Reactive oxygen species at phospholipid bilayers: distribution, mobility and permeation, Biochim. Biophys. Acta 1838 (2014) 438–444.
[22] S.J. Marrink, H.J.C. Berendsen, Simulation of water transport through a lipid membrane, J. Phys. Chem. 98 (1994) 4155–4168.
[23] S.J. Marrink, H.J.C. Berendsen, Free volume properties of a simulated lipid membrane, J. Phys. Chem. 100 (1996) 16729–16738.
[24] D. Poger, A.E. Mark, On the validation of molecular dynamics simulations of saturated and cis-monounsaturated Phosphatidylcholine lipid bilayers: a comparison with experiment, J. Chem. Theory Comput. 6 (2010) 325–336.
[25] D.K. Yadav, S. Kumar, E.H. Choi, P. Sharma, S. Misra, M. Kim, Insight into the molecular dynamic simulation studies of reactive oxygen species in native skin membrane, Front. Pharmacol. 9 (2018) 6030362.
[26] D.P.J. Van, E.C. Neyts, C.C.W. Verlackt, A. Bogaerts, Effect of lipid peroxidation on membrane permeability of cancer and normal cells subjected to oxidative stress, Chem. Sci. 7 (2016) 489–498.
[27] A.J.P. Netoa, R.M. Cordeiroa, Molecular simulations of the effects of phospholipid and cholesterol peroxidation on lipid membrane properties, Biochim. Biophys. Acta 1858 (2016) 2191–2198.
[28] J. Razzokov, M. Yusupov, S. Vanuytsel, E.C. Neyts, A. Bogaerts, Phosphatidylserine flip-flop induced by oxidation of the plasma membrane: a better insight by atomic scale modelling, Plasma Process. Polym. 14 (2017) 1700013.
[29] D.P.J. Van, C. Verheyen, E.C. Neyts, A. Bogaerts, Hampering effect of cholesterol on the permeation of reactive oxygen species through phospholipids bilayer: possible explanation for plasma Cancer selectivity, Sci. Rep. 7 (2017) 39526.
[30] C. Oostenbrink, T.A. Soares, N.F. Van, W.F. Gunsteren, Validation of the 53A6 GROMOS force field, Eur. Biophys. J. 34 (2005) 273.
[31] R. Andrade, E.G. Birgin, J.M. Martínez, A package for building initial configurations for molecular dynamics simulations, J. Comput. Chem. 30 (2010) 2157–2164.
[32] M. Swart, Density Functional Theory Applied to Copper Proteins Doctoral Dissertation, Rijksuniversiteit Groningen, 2002.
[33] J. Koput, S. Carter, N.C. Handy, Potential energy surface and vibrational − rotational energy levels of hydrogen peroxide, J. Phys. Chem. A 102 (1998) 6325–6330.
[34] P.C. Lee, M.A.J. Rodgers, Singlet molecular oxygen in micellar systems. 1. Distribution equilibriums between hydrophobic and hydrophilic compartments, J. Phys. Chem. 87 (1983) 4894–4898.
[35] V.S. Sokolov, P. Pohl, Membrane transport of singlet oxygen monitored by dipole potential measurements, Biophys. J. 96 (2009) 77–85.
[36] F. Fogolari, A. Corazza, S. Toppo, S.C.E. Tosatto, P. Viglino, F. Ursini, F. Esposito, Studying interactions by molecular dynamics simulations at high concentration, J. Biomed. Biotechnol. 9 (2012) 303190.
[37] W.G. Hoover, Lennard-Jones triple-point conductivity via weak external fields: additional calculations, Phys. Rev. A 31 (1985) 1695–1697.
[38] M. Parrinello, A. Rahman, Polymorphic transitions in single crystals: a new molecular dynamics method, J. Appl. Phys. 52 (1981) 7182–7190.
[39] M.P. Allen, D.J. Tildesley, Computer simulation of liquids, Physics Today, vol. 42, Clarendon Press, 1989, p. 99.
[40] D. Frenkel, B. Smit, Understanding Molecular Simulation: From Algorithms to Applications, 2nd ed., vol. 50, Academic Press, 1996, p. 66.
[41] J. Kästner, Umbrella sampling, WIRES Comput. Mol. Sci. 1 (2011) 932–942.
[42] J.S. Hub, B.L.D. Groot, D.V.D. Spoel, g_wham—a free weighted histogram analysis implementation including robust error and autocorrelation estimates, J. Chem. Phys. 6 (2015) 3713–3720.
[44] Matias Moller, Jack Lancaster, Ana Denicola, Chapter 2 the interaction of reactive oxygen and nitrogen species with membranes, Curr. Top. Membr. 61 (2008) 23–42.
[45] W.K. Subczynski, J.S. Hyde, Concentration of oxygen in lipid bilayers using a spin-label method, Biophys. J. 41 (1983) 283–286.
[46] S.T. Moin, T.S. Hofer, B.R. Randolf, B.M. Rode, An ab initio quantum mechanical charge field molecular dynamics simulation of hydrogen peroxide in water, Comput. Theor. Chem 980 (2012) 15–22.
[47] M. Laroussi, T. Akan, Arc-free atmospheric pressure cold plasma jets: a review, Plasma Process. Polym. 4 (2010) 777–788.
[48] G. Singh, A.C. Chamberlin, H.R. Zhekova, S.Y. Noskov, D.P. Tieleman, Two - dimensional potentials of mean force of Nile red in intact and damaged model bilayers. Application to calculations of fluorescence spectra, J. Chem. Theroy Comput. 12 (2015) 7–28.
[49] C.A. Fortier, B. Guan, R.B. Cole, M.A. Tarr, Covalently bound fluorescent probes as reporters for hydroxyl radical penetration into liposomal membranes, Free Radic. Biol. Med. 46 (2009) 1376–1385.
[50] B.H. Bielski, R.L. Arudi, M.W. Sutherland, A study of the reactivity of HO_2/O_2- with unsaturated fatty acids, J. Biol. Chem. 258 (1983) 4759–4761.
[51] H.W. Gardner, Lipid hydroperoxide reactivity with proteins and amino acids: a review, J. Agric. Food Chem. 27 (1979) 220–229.
[52] C. Christine Winterbourn, Reconciling the chemistry and biology of reactive oxygen species, Nat. Chem. Biol. 4 (2008) 278–286.
[53] R. Kohen, A. Nyska, Oxidation of biological systems: oxidative stress phenomena, antioxidants, redox reactions, and methods for their quantification, Toxicol. Pathol. 30 (2002) 620–650.
[54] J.C. Mathai, V. Sitaramam, Stretch sensitivity of transmembrane mobility of hydrogen peroxide through voids in the bilayer. Role of cardiolipin, J. Biol. Chem. 269 (1994) 17784–17793.